Analyst

Cite this: *Analyst*, 2011, **136**, 2495

www.rsc.org/analyst

PAPER

Gold nanoparticles in an ionic liquid phase supported in a biopolymeric matrix applied in the development of a rosmarinic acid biosensor

Daniela Brondani,*[a] Eduardo Zapp,[a] Iolanda Cruz Vieira,[a] Jairton Dupont[b] and Carla Weber Scheeren[b]

Received 20th January 2011, Accepted 27th March 2011
DOI: 10.1039/c1an15047b

Gold nanoparticles dispersed in 1-butyl-3-methylimidazolium hexafluorophosphate ionic liquid (Au-BMI·PF_6) were supported in chitin (CTN) chemically crosslinked with glyoxal and epichlorohydrin to obtain a new supported ionic liquid phase (SILP) catalyst with high catalytic activity, and providing an excellent environment for enzyme immobilization. This modified biopolymer matrix (Au-BMI·PF_6-CTN) was used as a support for the immobilization of the enzyme peroxidase (PER) from pea (*Pisum sativum*), and employed to develop a new biosensor for rosmarinic acid (RA) determination in pharmaceutical samples by square-wave voltammetry. In the presence of hydrogen peroxide, the PER catalyzes the oxidation of RA to the corresponding *o*-quinone, which is electrochemically reduced at a potential of +0.14 V *vs.* Ag/AgCl. Under optimized conditions, the resulting peak current increased linearly for the RA concentration range of 0.50 to 23.70 μM with a detection limit of 70.09 nM. The biosensor demonstrated high sensitivity, good repeatability and reproducibility, and long-term stability (15% decrease in response over 120 days). The method was successfully applied to the determination of RA content in pharmaceutical samples, with recovery values being in the range of 98.3 to 106.2%. The efficient analytical performance of the proposed biosensor can be attributed to the effective immobilization of the PER enzyme in the modified CTN matrix, the significant contribution of the high conductivity of the ionic liquid, the facilitation of electron transfer promoted by gold nanoparticles, and the inherent catalytic ability of these materials.

Introduction

Nanotechnology is regarded as an emerging technology, introducing new dimensions to science and technology, and it has multiple possible applications, involving various technological areas including advanced materials, biotechnology and medicine, electronics and scientific tools.[1] Great attention has been given to the application of nanostructured materials in biosensing systems, especially metallic nanoparticles (NPs).[2–5] The transition-metal NPs are playing an increasingly important role in the development of biosensors due to their unique properties, such as catalytic activity, high active surface area, size controllability and chemical stability. These promising materials have been extensively used in the construction of novel biosensors with enhanced performance in terms of miniaturization, biocompatibility, sensitivity, accuracy and stability.[2–6]

Ionic liquids (ILs) are liquid eletrolytes over a large range of temperatures, possess high ionic conductivity and catalytic ability, a large electrochemical window and high thermal and chemical stability.[7] These materials, especially imidazolium-derived salts, have proven to be suitable stabilizing agents for the generation and stabilization of metallic NPs. The IL forms a protective layer, which is probably composed of imidazolium aggregates located immediately adjacent to the surface of the metal NPs, promoting both steric and electronic protection against aggregation/agglomeration.[8,9] These metallic NPs stabilized in ILs have been used as novel materials for the construction of biosensors and electrochemical sensors with high analytical performance.[9–12]

More recently, a new technology, known as supported ionic liquid phase (SILP) catalysis, has emerged as an attractive alternative for the immobilization of catalytically active species (*e.g.*, metal complexes, metal NPs and enzymes).[9,13–18] The SILP catalysts form a new generation of heterogeneous catalysts, which combine the advantages of ILs with those of heterogeneous supported materials. This class of materials reduces considerably the amount of IL used and enables its reuse.[13,17] It can therefore be considered economically viable and environmentally benign. The SILP catalysts are prepared by the covalent attachment of the IL to the solid support surface or by simply depositing the IL phases (containing a catalyst or being the catalyst phase itself) onto the surface of the support, which is generally a material with high porosity and/or large surface area,

[a]*Department of Chemistry, Laboratory of Biosensors, Federal University of Santa Catarina, 88040-970 Florianópolis, SC, Brazil*
[b]*Institute of Chemistry, Laboratory of Molecular Catalysis, Federal University do Rio Grande do Sul, 91501-970 Porto Alegre, RS, Brazil*

such as silica, a clay mineral and a polymer.[9,13–18] In a study conducted by our group,[18] iridium NPs dispersed in 1-butyl-3-methylimidazolium tetrafluoroborate (Ir-BMI·BF_4) IL were supported in montmorillonite (MMT), to obtain a new SILP catalyst with high catalytic activity, and providing an excellent environment for enzymatic immobilization. This modified clay matrix (Ir-BMI·BF_4-MMT) was used for the immobilization of the laccase and polyphenol oxidase and successfully employed in the construction of a bi-enzymatic biosensor for determination of rutin by square-wave voltammetry (SWV), with a detection limit of 30.9 nM.

Different methods of enzymatic immobilization have been developed in order to improve or ensure the stability, selectivity and catalytic activity of these biomolecules, as well as reduce operating costs and enable reuse.[19–21] The characteristics of immobilized enzymes are controlled by the properties of both the enzyme and the support matrix. Several polymers have been used as the support material for immobilization of biocatalysts, such as alginate,[21–23] polyaniline,[24,25] chitosan[12,20,26,27] and chitin.[20,28,29] Of these materials, chitin (CTN) is notable for its excellent properties, such as chemical and physical stability, non-toxicity, biodegradability, bioactivity and biocompatibility, as well as high affinity with proteins, availability of reactive functional groups for direct reactions with enzymes and for chemical modifications.[20,30–33] CTN is a structural biopolymer, which has a role analogous to that of cellulose in terrestrial plants and collagen in the higher animals.[33] It is the most abundant natural amino polymer on earth, and occurs in nature as an important structural component in the exoskeleton of arthropods and in the cell walls of fungi and yeast.[32,33] Chemically, it is composed of β(1 → 4) linked 2-acetamido-2-deoxy-β-D-glucose units (or *N*-acetyl-D-glucosamine), forming a long-chain linear polymer.[20] Due to it providing an abundant resource with unquestionable advantages, CTN has attracted considerable attention from researchers, and has been efficiently applied as a support for the immobilization of enzymes.[20,28,29,31]

Enzymes have been extensively used in the development of biosensors, in particular the oxidoreductases, such as the peroxidases.[25,26,28,29,34,35] Peroxidases (PER) constitute a class of enzyme widely distributed in nature, and they can be easily obtained from the cells of various plants, animals and microorganisms. Most PER are heme proteins containing iron(III) protoporphyrin IX as the prosthetic group. Through the reduction of hydrogen peroxide they catalyze the oxidation of a wide variety of substrates, such as the phenolic compounds.[34–37]

Rosmarinic acid (RA), an ester of caffeic acid and 3,4-dihydroxyphenyllactic acid, is an important bioactive phenolic compound, which is commonly found in plants of the families Lamiaceae and Boraginaceae, which are used in the pharmaceutical and cosmetics industries. This phenolic compound carries out several pharmacological activities, such as antioxidant, anti-inflammatory, antimutagenic, antibacterial, antitumoral, hepatoprotective, cardioprotective and antiviral, besides acting as an astringent.[38–42] Thus, several analytical methods have been applied for RA determination, including capillary electrophoresis,[39,40] high-performance liquid chromatography,[41,43,44] spectrophotometry,[42] sensors and biosensors.[45–47] The development of biosensors has proven to be an attractive alternative to conventional methods, such as liquid chromatography, used for determination of phenolic compounds in several types of the samples. Some advantages of biosensors, relative to chromatographic techniques, are their fast response, good selectivity, cost-effectiveness, simplicity of construction and ease of surface renewal.

In this study, gold NPs dispersed in 1-butyl-3-methylimidazolium hexafluorophosphate IL (Au-BMI·PF_6) were supported in CTN chemically crosslinked with glyoxal and epichlorohydrin to obtain a new SILP catalyst with high catalytic activity, and providing an excellent environment for enzyme immobilization. PER from pea (*Pisum sativum*) was immobilized in the modified biopolymer matrix (Au-BMI·PF_6-CTN) and used to develop a novel biosensor for RA determination. Various experimental conditions were investigated in detail to obtain the best performance of the proposed method, such as the concentration of PER used in the biosensor construction, electrolyte support (buffer solution/pH), hydrogen peroxide concentration in the electrochemical measurements and SWV parameters (frequency, pulse amplitude and scan increment). The optimized biosensor was then applied to RA quantification in pharmaceutical samples by SWV.

Experimental

Chemicals, solutions and samples

All reagents were of analytical grade, used without further purification and all solutions were prepared with double-distilled water. Phosphate buffer solution (0.1 M, pH 7.0) was used as the supporting electrolyte. Rosmarinic acid (RA), guaiacol, hydrogen peroxide, ascorbic acid, benzoic acid, gallic acid, chlorogenic acid, esculetin, luteolin and rutin were purchased from Sigma-Aldrich. A standard solution of RA (0.50 mM) was prepared daily in phosphate buffer solution. Homogenate of pea (*Pisum sativum*) was used as a source of PER. The pea grains were purchased from a local producer in Florianópolis (Santa Catarina, Brazil), washed, chopped, and cooled in a refrigerator at 4 °C. Gold(III) chloride trihydate ($HAuCl_4 \cdot 3H_2O$, 99.9%) was purchased from Aldrich and used as a precursor for the preparation of Au-BMI·PF_6. CTN with an acetylation degree of 89.5% was purchased from Sigma Aldrich and used as the support for Au-BMI·PF_6, and for the enzymatic immobilization. Epichlorohydrin and glyoxal, used for the crosslinking of chitin, were obtained from Sigma. Graphite powder (Acheson 38, Fisher Scientific) and Nujol (Aldrich) of high purity were used in the preparation of the carbon paste. Three Brazilian pharmaceutical formulations containing RA (A, B and C = syrup based on spearmint extract (*Mentha crispa* L.)) were acquired from a local drugstore in Florianópolis (Santa Catarina, Brazil) and analyzed using the proposed biosensor.

Instrumentation

The morphology and the electron diffraction of the Au-BMI·PF_6 and Au-BMI·PF_6-CTN were observed on a JEOL JEM-2010 electron microscope equipped with an energy-dispersive X-ray spectroscopy system and a JEOL JEM-1200 EXII electron microscope operating at accelerating voltages of 120 kV. The X-ray diffraction (XRD) experiments were carried out on a SIEMENS D500 diffractometer equipped with a curved

graphite crystal using Cu-Kα R radiation (λ = 1.5406 Å). Scanning electron microscopy (SEM) and electron dispersive spectroscopy (EDS) analyses of the Au-BMI·PF_6-CTN were carried out using a JEOL model JSM 5800 with 10 and 20 kV.

The determination of PER activity was carried out using a B572 spectrophotometer (Micronal), with a quartz cell (optical path of 1.00 cm). The pH measurements were taken with a Micronal B475 pH-meter using a combined glass electrode. A Unique 1400A ultrasonic bath was used for preparation of the solutions.

Electrochemical measurements, using SWV and cyclic voltammetry (CV), were performed on an Autolab PGSTAT12 potentiostat/galvanostat (Eco Chemie, The Netherlands) connected to data processing software (GPES, software version 4.9.006, Eco Chemie). A conventional three-electrode system was used with a biosensor based on PER immobilized in the Au-BMI·PF_6-CTN matrix as the working electrode, a platinum wire as the counter electrode and an Ag/AgCl (3.0 M KCl) electrode as the reference electrode.

Crosslinking of the CTN using glyoxal and epichlorohydrin

Firstly, an excess of 4.0% (v/v) glyoxal solution prepared in phosphate buffer solution (0.1 M, pH 7.0) was transferred to a mass of 1.0 g CTN powder and mechanically stirred for 30 min at room temperature. After this reaction time, the CTN was washed with phosphate buffer solution (pH 7.0) to remove the excess of glyoxal, and dried at room temperature.[28,48] Then, 25.0 mL of 6.2 mM epichlorohydrin solution in phosphate buffer (pH 7.0) was added to the CTN and mechanically shaken for around 1 h at 50 °C. Subsequently, 7.0 mL of 0.1 M sodium hydroxide solution was added and the solution was boiled for at least 1 h. Soon after, the CTN was filtered and washed with 0.1 M hydrochloric acid and 0.1 M sodium hydroxide solutions, successively, to remove the excess of epichlorohydrin. Finally, the CTN was extensively washed with water and phosphate buffer solution (pH 7.0) to remove the excess of crosslinking reagents.[26,29,49] The chemically crosslinked CTN was dried at room temperature and stored in an well aired place for subsequent use as the support for Au-BMI·PF_6 and pea PER immobilization.

Synthesis and characterization of Au-BMI·PF_6

Initially, a solution was prepared by dissolving $NaBH_4$ (9.25 mg, 250 mmol) in 0.5 mL of methanol, and subsequent dispersion in 0.5 mL of BMI·PF_6 IL, 24 h before use. In a Schlenk tube, the Au NPs precursor $HAuCl_4 \cdot 3H_2O$ (10 mg, 25 mmoL) dissolved in 0.5 mL of methanol and 0.5 mL of BMI·PF_6 IL were stirred at room temperature for 15 min, yielding a yellow solution. Then, 1-methylimidazole (0.005 mg, 0.06 mmol) was added in the solution and stirred. Subsequently, the solution containing $NaBH_4$ (previously prepared) was also added to the solution in a Schlenk tube, and a blue "solution" was obtained and dried under reduced pressure.[50] The Au NPs were isolated by centrifugation (3500 rpm) with the addition of acetone (5 mL) for 3 min and washed with acetone (3 × 15 mL) and dichloromethane (3 × 15 mL), dried under reduced pressure and isolated. The Au-BMI·PF_6 samples thus obtained were prepared for TEM and X-ray analysis.

The phase structures of the Au-BMI·PF_6 were characterized by XRD. For this analysis, the Au NPs were isolated as a fine powder and placed in the sample holder. The diffraction data were collected at room temperature in a Bragg-Brentano θ–2θ geometry. The equipment was operated at 40 kV and 20 mA with a scan range of between 20° and 90°. The diffractograms were obtained with a constant step, $\Delta 2\theta$ = 0.05. The indexation of Bragg reflections was obtained by a pseudo-Voigt profile fitting using the FULLPROF code.[51]

The samples for transmission electron microscopy (TEM) analysis were prepared by dispersion of the Au-BMI·PF_6 at room temperature and then collected on a carbon-coated copper grid. The histogram of the Au NPs size distribution was obtained from measurements of around 300 diameters and was reproduced in different regions of the Cu grid.[52]

Preparation and characterization of Au-BMI·PF_6 supported in crosslinked CTN

The biopolymeric suspension was prepared by dispersing 1.0 g of CTN (previously crosslinked) in a 100 mL of distilled water, and the pH of this suspension was adjusted to 9–10 by adding NaOH solution. A further dispersion was carried out by ultrasonic treatment for 15 min.[53] For the preparation of the CTN suspension containing Au NPs and IL, 10 mg of Au-BMI·PF_6 (previously prepared) were added to 20 mL of CTN suspension, and the mixture was dispersed by sonication for 15 min. The suspension obtained, consisting of the Au NPs and IL supported in CTN (Au-BMI·PF_6-CTN), was isolated by centrifugation (3500 rpm) for 3 min, washed with hexane (3 × 5 mL) and dried under reduced pressure. The Au-BMI·PF_6-CTN samples thus obtained were prepared for TEM analysis, depositing the particles directly on the holey carbon film supported on a copper grid. This material was also characterized by SEM and EDS analyses, using a magnification of 1250×.

Obtainment of the PER and measurement of activity

The PER enzyme was obtained from pea (*P. sativum*) according to the following methodology: 25 g of the pea grains were homogenized in a blender with 100 mL of phosphate buffer solution (0.1 M, pH 7.0) until total homogenization of the extract, at low temperature (4 °C) to preserve the enzymatic activity. The homogenate obtained was then rapidly filtered to eliminate the solid tissue and stored in a refrigerator (4 °C) for subsequent use as the PER source.[28,29]

The activity of PER present in the pea homogenate was determined in triplicate by measuring the absorbance at 470 nm of tetraguaiacol produced by the reaction between 0.2 mL of plant homogenate, 2.7 mL of 50 mM guaiacol solution and 0.1 mL of 9.8 mM hydrogen peroxide solution in phosphate buffer (0.1 M, pH 7.0) at room temperature.[28,29]

Immobilization of PER in Au-BMI·PF_6-CTN matrix

The immobilization of the PER in the CTN matrix containing Au-BMI·PF_6 was performed through the following procedure: aliquots (30–125 μL) of pea homogenate, containing 500 to

2000 units of PER, were added to 20 mg of the modified CTN matrix (Au-BMI·PF_6-CTN), individually. A paste was obtained after homogenization with a spatula (5 min) and then dried at room temperature. The resulting material containing Au-BMI·PF_6 and PER immobilized in crosslinked CTN was used for construction of the proposed biosensor.

Construction of the biosensor

Firstly, 140 mg of graphite powder (70%, w/w) and 20 mg of Au-BMI·PF_6-CTN containing 1500 units of PER (10%, w/w) were homogenized for 15 min with a mortar and pestle. Subsequently, 40 mg of Nujol (20%, w/w) were added to the mixture which was then homogenized for a total of 15 min. After complete homogenization, the graphite paste obtained was compacted into a plastic tip with 1.0 mm internal diameter. Finally, a copper wire of dimensions 0.4 cm × 5.0 cm was introduced for the electrical contact and the biosensor was then used as the working electrode. The biosensors containing PER immobilized on crosslinked CTN (without Au-BMI·PF_6 supported) and free enzyme were prepared following the same steps. The bare carbon paste electrode (bare CPE) was prepared in a similar way by mixing only graphite powder and Nujol in a mortar. The constructed electrodes were stored at room temperature in a dry place when not in use.

Electrochemical measurements

All SWV and CV measurements were performed at room temperature (25 ± 0.5 °C) in a glass electrochemical cell containing a 10.0 mL aliquot of phosphate buffer solution (0.1 M, pH 7.0) not deaerated, and successive additions of an RA standard solution or a pharmaceutical sample were carried out using a micropipette. The SWV measurements were carried out applying a potential sweep between +0.50 and −0.20 V at a frequency of 10–120 Hz, pulse amplitude of 10–100 mV and scan increment of 1.0–10.0 mV, after successive additions of the analyte. The cyclic voltammograms were recorded by cycling the potential between +0.65 and −0.60 V at a scan rate of 200 mV s^{-1}. All measurements were registered *vs.* Ag/AgCl (3.0 M KCl), and with a stirring time of 60 s to homogenize the solutions.

Analysis of the pharmaceutical samples

The quantification of RA using the proposed biosensor was performed by the method of standard addition. Aliquots of 50 μL of the pharmaceuticals samples (A, B and C = syrup based on spearmint extract) were directly transferred to the electrochemical cell containing 10,0 mL of the supporting electrolyte (phosphate buffer, 0.1 M, pH 7.0) and 50 μL of the hydrogen peroxide solution (9.79 mM), and successive additions of RA standard solution were carried out using a micropipette. After each addition, the solution was stirred for 60 s and SWV measurements were recorded by scanning the potential from +0.50 to −0.20 V *vs.* Ag/AgCl at a frequency of 100 Hz, pulse amplitude of 80 mV and scan increment of 8.0 mV. All measurements were performed in triplicate and the quantification was based on the current resulting from the RA.

Results and discussion

Characterization of Au-BMI·PF_6 and Au-BMI·PF_6 supported in CTN

The XRD analysis clearly identified crystalline Au in the Au-BMI·PF_6 sample and indicated that the mean diameter (d_m ≈ 11 ± 0.3 nm) could be estimated from the XRD pattern by means of the Debye-Scherrer equation calculated from full width at half-maximum (fwhm) of the (111), (200), (220), (311) and (222) reflection planes (Fig. 1).

The TEM analysis was performed with samples prepared using Au-BMI·PF_6 and Au-BMI·PF_6-CTN. The Au-BMI·PF_6 sample was shaken ultrasonically and then deposited on holey carbon film supported by a copper grid, while the Au-BMI·PF_6-CTN sample was deposited directly onto this surface for analysis. The grids were placed on filter paper to remove the excess material and allowed to dry out for 2 h under high vacuum. Finally, these TEM samples were examined using a JEM-2010 microscope operating at an accelerating voltage of 120 kV. Bright field TEM observations were performed under slight underfocus conditions (Δf ≈ −300 nm), and particle size distributions of the Au NPs were determined once the original negative had been digitalized and expanded to 470 pixels cm^{-1}. The TEM micrograph of Au-BMI·PF_6 (Fig. 2-A) and Au-BMI·PF_6 supported in CTN (Fig. 2-B) was observed at 120 kV with a magnification of 500 K and an underfocus of 500 nm, where the Au NPs are represented by black points. As can be seen in Fig. 2-B, the metallic NPs were heterogeneously distributed in the modified CTN matrix. The particles display an irregular shape, but evaluation of their characteristic diameter results in a monomodal particle size distribution. The mean diameter (d_m ≈ 11 ± 0.3 nm) of the Au NPs dispersed in BMI·BF_6 was estimated from ensembles of 300 particles, found in an arbitrarily chosen area of the enlarged micrographs. Fig. 2-C shows the particle size distributions obtained, which can be reasonably well fitted by a Gaussian curve.

The SEM analysis of Au-BMI·PF_6-CTN confirmed the presence and dispersion of the Au-BMI·PF_6 supported in the crosslinked CTN matrix used for enzymatic immobilization. Also, the metal distribution determined by SEM-EDS analysis showed the presence of metal gold (data not shown).

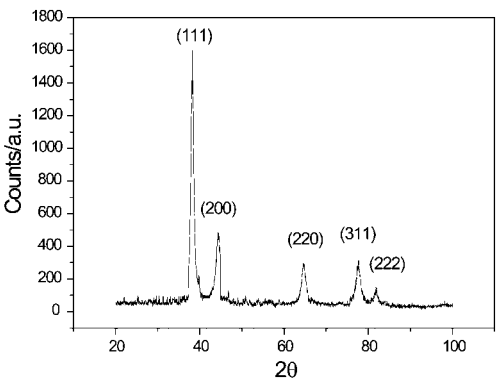

Fig. 1 XRD pattern for the Au-BMI·PF_6.

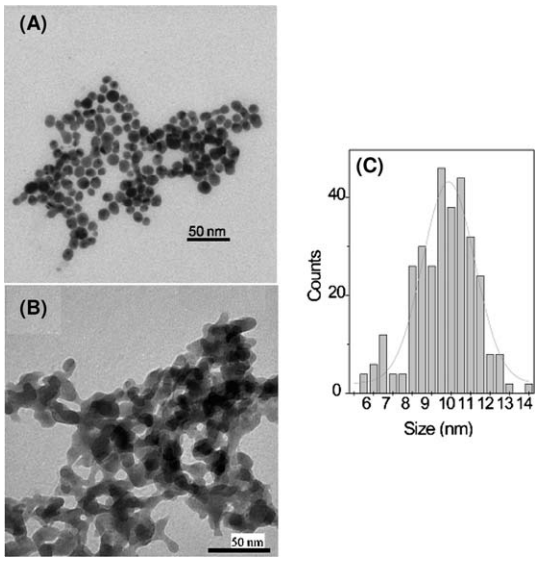

Fig. 2 TEM micrograph showing the Au NPs in (A) Au-BMI·PF_6 and (B) Au-BMI·PF_6-CTN samples (Au NPs represented by the black points) observed at 120 kV with a magnification of 500 K and an underfocus of 500 nm. (C) Histogram illustrating the particle size distribution.

Crosslinked CTN containing Au-BMI·PF_6 and immobilized PER

The properties of immobilized enzymes are controlled by the characteristics of both the enzyme and the support material. CTN is an excellent support material for enzyme immobilization because of its various characteristics including hydrophilicity, biocompatibility, biodegradability and physicochemical stability. Moreover, the presence of acetamido groups and free amino and hydroxyl groups in CTN is highly advantageous for making available distinctive biological functions and conducting reactions to modify its chemical structure.[20,28,30]

Fig. 3 shows a proposed scheme for the immobilization of PER on CTN crosslinked with glyoxal and epichlorohydrin. Initially, the glyoxal was used for the activation of the amine groups of the CTN (approximately 10.5%). Glyoxal induces Schiff's base formation between its aldehyde groups and amino groups of the enzyme molecules. The subsequent addition of the epichlorohydrin causes rupture of the epoxide ring linking through the carbon atom and removal of the chloride atom. An IL phase containing Au NPs was supported in the crosslinked CTN, and subsequently the pea homogenate containing the PER enzyme was added to this biopolymeric matrix. It is possible that the PER is covalently immobilized and entrapped within the interstitial space of the crosslinked CTN biopolymer providing strong interactions and high stability. In addition, the crosslinked CTN containing Au-BMI·PF_6 forms a favorable microenvironment around the enzymes, making this method more efficient in terms of maintaining the stability and extending the lifetime of these biomolecules.

Principle of the enzymatic process occurring on the biosensor

Reactions catalyzed by enzymes have been widely used in the determination of various analytes in the pharmaceutical, environmental and food areas.[12,26,28,29,54–57] PER catalyzes the oxidation of several phenolic compounds to the corresponding quinones in the presence of hydrogen peroxide. The development of biosensors based on PER from plant extract or tissue has been reported in the literature[26,28,29,54] and they showed high stability, high enzyme activity, ease of obtainment and low cost in comparison with electrodes constructed with purified enzymes.

Fig. 4 shows a scheme of the reaction involved in the oxidation of RA catalyzed by PER on the electrode surface. Initially, RA in contact with PER, in the presence of the hydrogen peroxide, is oxidized to the corresponding *o*-quinone. Subsequently, the quinone produced is electrochemically reduced on the biosensor surface at a potential of +0.14 V *vs.* Ag/AgCl. The resultant current obtained in the electrochemical reduction of *o*-quinone to the initial compound (RA) is proportional to the analyte concentration and was used for quantification of this phenolic compound.

Voltammetric behavior of RA in the bare CPE and biosensors

An evaluation of the contribution of the components employed in the construction of the biosensor was carried out. In previous studies carried out by our group[18,28] the best carbon paste electrode composition was found to be the ratio 70 : 20 : 10% (w/w) graphite powder:binder:modifier material. Therefore, this carbon paste composition was used in the present study in the construction of the biosensor using different modifier materials. Fig. 5 shows the cyclic and square-wave voltammograms obtained using the (a) bare CPE, (b) biosensor-PER (free enzyme), (c) biosensor-PER-CTN, (d) biosensor-PER-Au-BMI·PF_6-CTN (c and d – immobilized enzyme).

The CV measurements (Fig. 5-A) were performed in phosphate buffer solution (0.1 M, pH 7.0) containing 48.7 μM hydrogen peroxide and 0.75 mM RA. It can be observed that the successive addition of material modifier to the carbon paste causes significant changes in the behavior and performance of the electrodes, leading to an improvement in the analytical response. The background current observed in the response of the biosensor (d) is due to the capacitance of the electrode, and was attributed to the presence of the IL in the modified material (Au-BMI·PF_6-CTN). With the addition of IL and metal NPs to the CPEs the rate of transfer charge increases, due to the higher conductivity of the electrode containing these modifiers.

All SWV measurements (Fig. 5-B) were performed in phosphate buffer solution (0.1 M, pH 7.0) containing 48.7 μM hydrogen peroxide and 16.80 μM RA. Through this study, the contribution of each modifier material to the resulting currents obtained using the biosensors for RA detection can be seen more clearly. In relation to the bare CPE (a), the addition of PER to the electrode (b) promotes an increase of approximately 35% in the response due to the catalytic activity of the enzyme toward RA oxidation. The response obtained using the biosensor (c), which contains the immobilized PER in crosslinked CTN, was 24% higher than that of the electrode (b) containing free enzyme. The biosensor (d) showed a peak current approximately 26% higher than that of the electrode (c), due to the catalytic activity of the immobilized PER, together with the facilitation of electron transfer provided by the addition of the biopolymer modified with Au NPs and IL. This investigation demonstrates the benefits

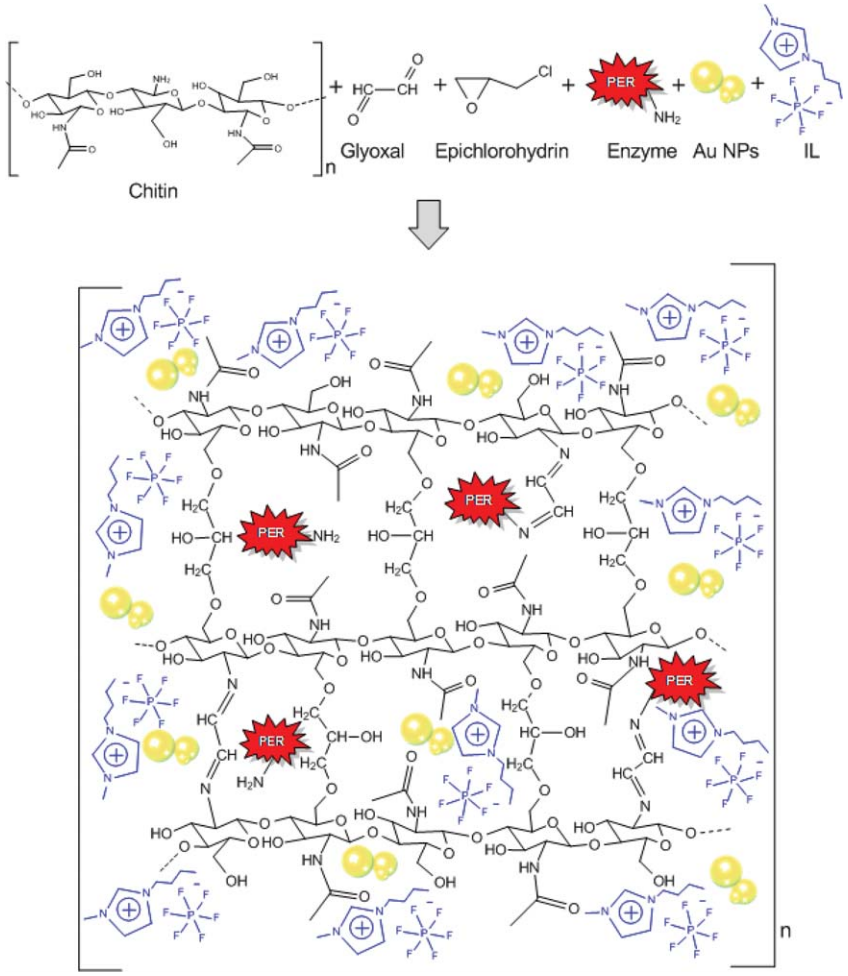

Fig. 3 Schematic illustration of Au-BMI·PF_6 and PER immobilized on CTN crosslinked with glyoxal and epichlorohydrin.

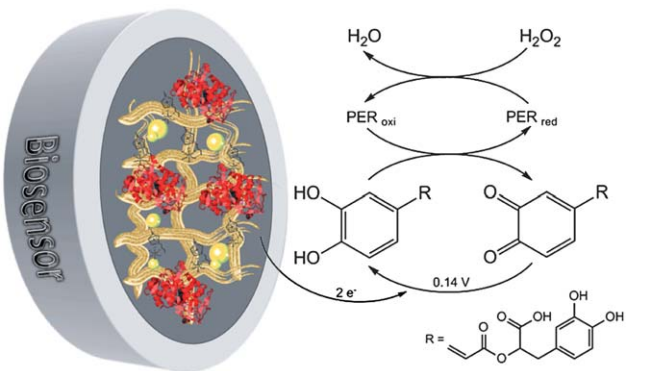

Fig. 4 Schematic representation of the PER-catalyzed oxidation of RA with its subsequent electrochemical reduction on the biosensor surface, in the presence of hydrogen peroxide.

of incorporating these modifiers, particularly the new modified polymeric matrix containing Au NPs and IL, for the development of biosensors with greater sensitivity. Besides the intrinsic catalytic ability of the metallic NPs and IL, the presence of these materials can also provide a suitable microenvironment for the enzyme, allowing the direct transfer of electrons between the immobilized enzyme and the electrode surface. This behavior is in agreement with studies performed with biosensors containing Ir-BMI·BF_4,[18] Pt-BMI·PF_6,[11] Ag-BMI·PF_6 and Au-BMI·PF_6.[12]

Thus, considering that biosensor (d) presented the highest analytical response in the study carried out, this electrode was selected for the biosensor optimization and applied to the determination of RA in real samples.

Optimization of the biosensor construction and experimental conditions

Various experimental conditions were thoroughly investigated in the optimization of the proposed method, in the search for the best analytical response and peak definition, such as the concentration of PER used in the biosensor construction, electrolyte support (buffer solution/pH), hydrogen peroxide concentration in the electrochemical measurements and the SWV parameters (frequency, pulse amplitude and scan increment).

The effect of the concentration of PER in the preparation of the electrode was investigated from 3.3 to 13.3 units of PER/mg of carbon paste, using pea homogenate as the enzymatic source. The best response was obtained with the use of 7.5 units of PER/mg of carbon paste, and with a higher amount of PER a decrease in the analytical response was observed. This result is consistent

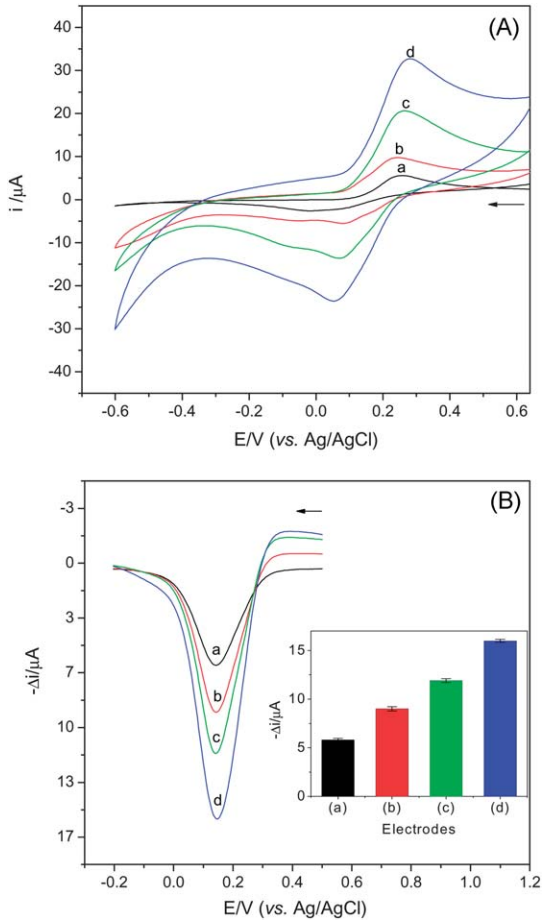

Fig. 5 (A) Cyclic and (B) square-wave voltammograms obtained using the (a) bare CPE, (b) biosensor-PER (free enzyme), (c) biosensor-PER-CTN, (d) biosensor-PER-Au-BMI·PF_6-CTN (c and d – immobilized enzyme) in phosphate buffer solution (0.1 M, pH 7.0) containing 48.7 μM hydrogen peroxide and (A) 0.75 mM RA at 200 mV s^{-1} and (B) 16.80 μM of RA at frequency 100 Hz, pulse amplitude 80 mV and scan increment 8.0 mV. Inset: Current values for bare CPE and different biosensors.

with another study conducted in our group, in which a biosensor was constructed using PER obtained from corn.[28] Therefore, the enzymatic concentration of 7.5 units of PER/mg of carbon paste was used to continue the optimization studies.

The use of an appropriate supporting electrolyte is extremely important in electrochemical processes. A study to select the best pH of the supporting electrolyte for the proposed method was carried out using 0.1 M phosphate buffer solutions under different pH conditions (6.0, 6.5, 7.0, 7.5, and 8.0). The highest current intensity for RA determination was obtained using phosphate buffer solution pH 7.0 and, consequently, this supporting electrolyte was selected for the subsequent analyses. This result is in agreement with other studies using plant-derived PER reported in the literature.[26,28,29,58]

The hydrogen peroxide concentration (from 9.8 to 192.0 μM) used in the electrochemical measurements and its influence on the biosensor response were also investigated. The optimum hydrogen peroxide concentration was found to be 48.7 μM. Therefore, this concentration was selected for subsequent studies.

Finally, the SWV parameters were investigated and optimized to obtain the best biosensor performance. The parameters and ranges investigated were: frequency (10–120 Hz), pulse amplitude (10–120 mV) and scan increment (1–10 mV). This study was performed in phosphate buffer solution (0.1 M, pH 7.0) containing 48.7 μM hydrogen peroxide and 4.93 μM RA, and the best analytical response was obtained using a frequency of 60 Hz, amplitude of 100 mV and scan increment of 5 mV. Thus, these instrumental conditions were selected for all subsequent RA determinations.

Stability, repeatability and reproducibility of the biosensor

The stability was investigated to evaluate the performance of the biosensor and the efficiency of the enzyme immobilization. For this study, the biosensor was tested for the determination of RA at different intervals over a period of approximately 120 days stored at room temperature. In relation to the response obtained on the day of construction, a relative response of more than 96.1% was maintained during the first 30 days, and after a period of 60 and 120 days the biosensor exhibited a relative response of 90.5 and 85.0%, respectively. These results are acceptable and can be attributed to preservation of the integrity of the PER which maintained its enzymatic activity due to its immobilization in the Au-BMI·PF_6-CTN matrix.

The repeatability study was carried out through ten successive measurements by SWV, using the proposed biosensor in 4.93 μM of RA in phosphate buffer solution (0.1 M, pH 7.0). The biosensor showed a relative standard deviation (RSD) of 2.7% for this study. The reproducibility of the analytical signal for RA was observed using six biosensors constructed individually, under the previously optimized conditions. An adequate reproducibility was obtained, with an RSD of the current values of 4.9%.

Square-wave voltammograms and analytical curve

The construction of the analytical curve for RA was performed using the proposed biosensor by SWV, under the previously optimized experimental conditions, in the potential range of +0.50 to −0.20 V *vs.* Ag/AgCl. The electrochemical reduction of RA on the surface of the biosensor was obtained at a potential of approximately +0.14 V *vs.* Ag/AgCl. The representation of square-wave voltammograms used to obtain the calibration curve for RA is shown in Fig. 6. The regression equation for the analytical curve is as follows: $-\Delta i = 1.75(\pm 0.02) + 8.56(\pm 0.03) \times 10^5$ [RA], with a correlation coefficient (R) of 0.9993, where Δi is the resultant peak current (μA) and [RA] is the RA concentration (M). The linear range obtained was 0.50 μM to 23.70 μM of RA. The calculated limit of detection (LOD = three times the standard deviation of the intercept/slope) and limit of quantification (LOQ = ten times the standard deviation of the intercept/slope) were found to be 70.09 nM and 0.23 μM, respectively.

This biosensor showed lower detectability for RA in comparison to another biosensor previously developed by our group.[45] The biosensor constructed by Franzoi *et al.*[45] was based on laccase from *Aspergillus oryzae* and BMI·PF_6 IL, and presented a linear range to RA concentrations of 0.99 μM to 65.40 μM with a LOD of 0.19 μM. In addition, the biosensor that we are now proposing is more sensitive than that another biosensor[45] (slope = 5.63×10^5 μA M^{-1}). Thus, the satisfactory

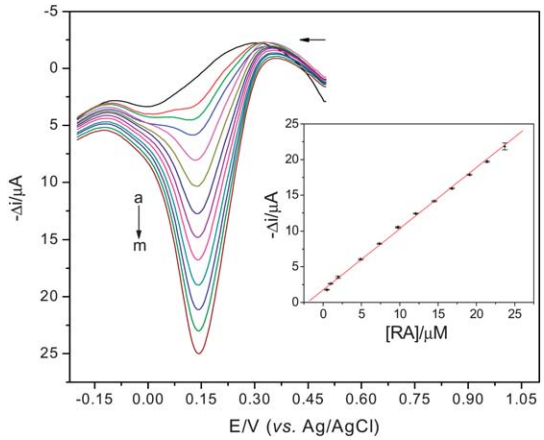

Fig. 6 Square-wave voltammograms obtained using the proposed biosensor in (a) 48.7 μM hydrogen peroxide in phosphate buffer solution (0.1 M, pH 7.0) and standard solutions of RA in the following concentrations: (b) 0.50 μM, (c) 0.99 μM, (d) 1.98 μM, (e) 4.93 μM, (f) 7.35 μM, (g) 9.76 μM, (h) 12.10 μM, (i) 14.50 μM, (j) 16.80 μM, (k) 19.10 μM, (l) 21.40 μM, and (m) 23.70 μM at frequency 100 Hz, pulse amplitude 80 mV and scan increment 8.0 mV. Inset: analytical curve of RA.

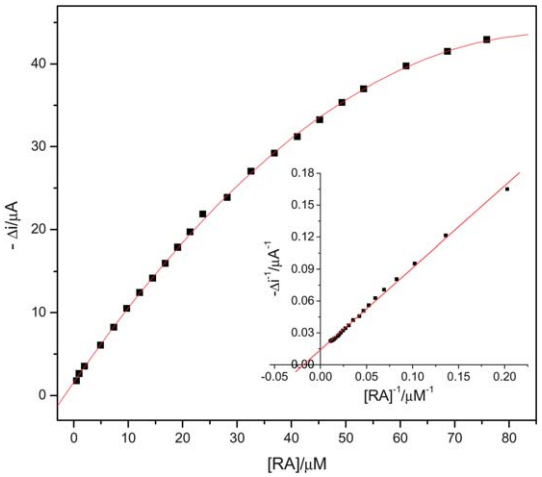

Fig. 7 Current response of the proposed biosensor obtained by SWV as a function of RA concentration. Insert: Lineweaver–Burk plot of the data.

performance of the proposed biosensor can be attributed to the good stability of the immobilized PER, high conductivity of the IL and facilitation of the electron transfer by the Au NPs, significantly improving the detectability of the electrode. A notable contribution of the IL and Au NPs supported in CTN to the analytical response of the biosensor can be seen in Fig. 5 (shown previously), confirming the capacity of these materials to improve the detectability and sensitivity of this method.

Determination of the Michaelis–Menten constant

The apparent Michaelis–Menten constant (K_m^{app}), which gives an indication of the enzyme–substrate kinetics, can be obtained from the electrochemical version of the Lineweaver–Burk model (double reciprocal).[59] The parameter K_m^{app} is inversely proportional to the affinity of the enzyme for the substrate.[60] To obtain the K_m^{app} value, the proposed biosensor (biosensor-PER-Au-BMI·PF_6-CTN) was employed in the determination of RA in concentrations of 0.50 to 75.90 μM in phosphate buffer solution (0.1 M, pH 7.0) containing 48.7 μM hydrogen peroxide at 25 ± 0.5 °C. Fig. 7 shows the current response of the proposed biosensor obtained by SWV as a function of RA concentration. As can be seen, at high RA concentrations the resulting peak current deviated from linearity and approached a constant value reflecting the maximum rate of the enzymatic reaction under RA saturation conditions, showing a characteristic of Michaelis–Menten kinetic mechanism. The K_m^{app} value was determined using the Lineweaver–Burk plot ($1/\Delta i$ *vs.* 1/[RA]), where the intercept with the *x*-axis is equal to $-1/K_m^{app}$,[59] and a value of 54.8 μM was obtained. This small K_m^{app} value indicates that the biosensor-PER-Au-BMI·PF_6-CTN has high catalytic efficiency in the RA determination. This study was also conducted with the biosensor containing free enzyme (biosensor-PER – electrode "b" shown in Fig. 5) and the biosensor containing immobilized enzyme in crosslinked CTN (biosensor-PER-CTN – electrode "c" shown in Fig. 5), and the values of 407.4 μM and 263.0 μM were found, respectively. The smaller K_m^{app} value means that the immobilized enzyme has higher enzymatic activity, even after the immobilization process.[59,61,62] Therefore, the results of this study showed that the immobilization procedure promoted a significant increase in the enzyme selectivity toward RA.

Interference, recovery study and analytical application

Some compounds with electroactive properties may be potential interferents in terms of the analytical response when present in the pharmaceutical samples under analysis. Thus, in this study, using the proposed biosensor, the possibly interference from various compounds present in the drug samples in the analytical signal obtained in RA determination was investigated in detail. The compounds investigated were ascorbic acid, benzoic acid, esculetin, luteolin, rutin, chlorogenic acid and gallic acid. SWV measurements were performed using solutions containing 4.93 μM of RA in phosphate buffer solution (0.1 M, pH 7.0) and adding different concentrations of the above-mentioned compounds. The ratios between the concentrations of RA and each interfering compound were fixed at 1 : 1, 1 : 2, 1 : 3, 1 : 5 and 1 : 10. The interference study was performed in triplicate and the results indicated that the compounds tested showed no significant interference in the analysis, causing changes in the analytical signal for RA of less than ±3.0% for a concentration ratio of 1 : 1 and less than ±6.5% for ratios of 1 : 3 using luteolin, rutin and chlorogenic acid and 1 : 10 using the other potentially interfering compounds studied (Table 1). These results indicate that this electrode was able to determine the amount of RA in the presence of the potential interferents with good selectivity.

A recovery study and RA determination were performed with the standard addition method, in triplicate, using three pharmaceutical samples (A, B and C). Recovery measurements were obtained by adding different standard concentrations (4.90, 9.71 and 14.40 μM) of RA to each pharmaceutical sample. The percentage recovery values were calculated by comparing the concentrations detected in samples with and without the addition

Table 1 Study of potentially interfering compounds in quantification of RA using the proposed biosensor

Compound (C)	Structure	[RA]:[C]	Change in the analytical signal of RA (%)[a]
ascorbic acid	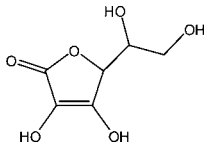	1 : 1 1 : 5 1 : 10	1.11 ± 0.1 3.70 ± 0.2 5.55 ± 0.1
benzoic acid	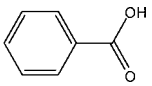	1 : 1 1 : 5 1 : 10	0.92 ± 0.3 2.24 ± 0.1 3.56 ± 0.1
esculetin	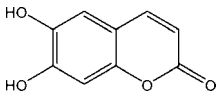	1 : 1 1 : 5 1 : 10	0.35 ± 0.2 3.85 ± 0.2 6.47 ± 0.1
luteolin	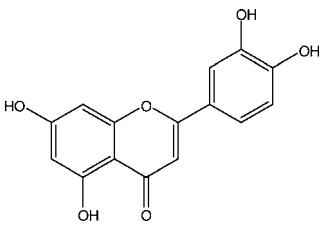	1 : 1 1 : 2 1 : 3	2.86 ± 0.3 4.28 ± 0.1 5.71 ± 0.2
rutin	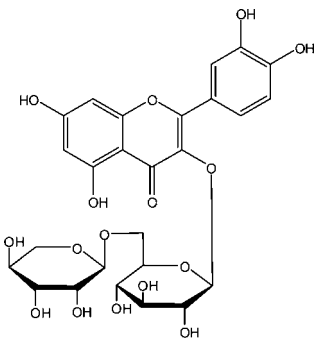	1 : 1 1 : 2 1 : 3	2.53 ± 0.1 5.06 ± 0.1 6.33 ± 0.2
chlorogenic acid	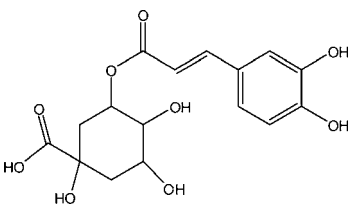	1 : 1 1 : 2 1 : 3	1.45 ± 0.2 2.90 ± 0.1 5.80 ± 0.2
gallic acid	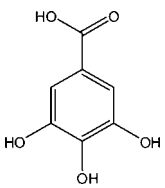	1 : 1 1 : 5 1 : 10	2.11 ± 0.1 3.74 ± 0.2 5.20 ± 0.1

[a] Mean ± standard deviation; $n = 3$.

of known concentrations of the RA standard solution. The recoveries of 98.4 to 106.3% obtained for these samples demonstrate the satisfactory accuracy of the proposed biosensor (Table 2). It can be clearly observed that the recovery results obtained indicate an absence of matrix effects in the analysis.

In addition, to verify the efficiency of the biosensor developed, these pharmaceutical samples were also used in the RA quantification. The RA contents determined in samples A, B and C were 1.77 ± 0.001, 1.80 ± 0.001 and 1.72 ± 0.002 mM, respectively. These contents of RA obtained using the biosensor are consistent with the content specified on the label of the pharmaceutical formulations (1.79 mM), with a relative error of less than ±3.9%, confirming the accuracy of the method proposed in this study.

Table 2 Recovery of RA in pharmaceutical samples using the proposed biosensor

	RA (μM)		
Sample[a]	Added	Found[b]	Recovery (%)[c]
A	4.90	4.90 ± 0.25	100.0
	9.71	9.90 ± 0.19	102.0
	14.40	14.29 ± 0.17	99.2
B	4.90	5.21 ± 0.19	106.3
	9.71	9.65 ± 0.11	99.4
	14.40	14.40 ± 0.22	100.0
C	4.90	4.82 ± 0.19	98.4
	9.71	9.96 ± 0.14	102.6
	14.40	14.29 ± 0.22	99.2

[a] A, B and C = syrup based on spearmint extract. [b] Mean ± standard deviation; $n = 3$. [c] Recovery = (mean value found/added value) × 100.

Conclusions

This paper describes the synthesis of a new SILP catalyst based on Au NPs and IL (Au-BMI·PF_6) supported in CTN chemically crosslinked with glyoxal and epichlorohydrin, and its application as an excellent matrix for enzyme immobilization. This modified biopolymer matrix (Au-BMI·PF_6-CTN) was used as a support for the immobilization of the enzyme PER obtained from pea, and employed to develop a new biosensor for RA quantification in pharmaceutical samples by SWV. This biosensor exhibited high sensitivity, adequate selectivity, and good reproducibility and stability. In addition, the cost-effectiveness and simplicity of the proposed biosensor makes it superior to other traditional analytical methods used for phenolic compounds determination. The efficient analytical performance of the proposed biosensor can be attributed to the effective immobilization of the PER enzyme in the modified CTN matrix, the significant contribution of the high conductivity of IL BMI·PF_6, the facilitation of electron transfer promoted by Au NPs, and the inherent catalytic ability of the IL and metallic NPs. A significant contribution of these modifier materials was observed in the study described herein, especially in relation to an increase in the current responses obtained with the proposed biosensor compared to an unmodified electrode. The results of this study show that the proposed method offered good precision and accuracy for the determination of RA in pharmaceutical formulations.

Acknowledgements

Financial support from CNPq (Processes 472169/2004-1 and 472541/2006-4), MCT/CNPq/PADCT, and also the scholarships granted by CNPq to DB and EZ are gratefully acknowledged.

References

1 K. Miyazaki and N. Islam, *Technovation*, 2007, **27**, 661–675.
2 A. Merkoçi, *Biosens. Bioelectron.*, 2010, **26**, 1164–1177.
3 C. Jianrong, M. Yuqing, H. Nongyue, W. Xiaohua and L. Sijiao, *Biotechnol. Adv.*, 2004, **22**, 505–518.
4 I. Willner, B. Willner and R. Tel-Vered, *Electroanalysis*, 2011, **23**, 13.
5 X. Zhang, Q. Guo and D. Cui, *Sensors*, 2009, **9**, 1033–1053.
6 S. Vaddiraju, I. Tomazos, D. J. Burgess, F. C. Jain and F. Papadimitrakopoulos, *Biosens. Bioelectron.*, 2010, **25**, 1553–1565.
7 J. Dupont, *J. Braz. Chem. Soc.*, 2004, **15**, 341–350.
8 P. Migowski and J. Dupont, *Chem.–Eur. J.*, 2007, **13**, 32–39.
9 J. Dupont and J. D. Scholten, *Chem. Soc. Rev.*, 2010, **39**, 1780–1804.
10 D. Brondani, I. C. Vieira, C. Piovezan, J. M. R. da Silva, A. Neves, J. Dupont and C. W. Scheeren, *Analyst*, 2010, **135**, 1015–1022.
11 D. Brondani, C. W. Scheeren, J. Dupont and I. C. Vieira, *Sens. Actuators, B*, 2009, **140**, 252–259.
12 A. C. Franzoi, I. C. Vieira, J. Dupont, C. W. Scheeren and L. F. Oliveira, *Analyst*, 2009, **134**, 2320–2328.
13 G. Rashinkar and R. Salunkhe, *J. Mol. Catal. A: Chem.*, 2010, **316**, 146–152.
14 Y. Jiang, C. Guo, H. Xia, I. Mahmood, C. Liu and H. Liu, *J. Mol. Catal. B: Enzym.*, 2009, **58**, 103–109.
15 S. Werner, N. Szesni, A. Bittermann, M. J. Schneider, P. Härter, M. Haumann and P. Wasserscheid, *Appl. Catal., A*, 2010, **377**, 70–75.
16 A. Riisager, R. Fehrmann, M. Haumann and P. Wasserscheid, *Top. Catal.*, 2006, **40**, 91–102.
17 M. A. Gelesky, C. W. Scheeren, L. Foppa, F. A. Pavan, S. L. P. Dias and J. Dupont, *Biomacromolecules*, 2009, **10**, 1888–1893.
18 E. Zapp, D. Brondani, I. C. Vieira, J. Dupont and C. W. Scheeren, *Electroanalysis*, 2011, **23**, 764–776.
19 C. Mateo, J. M. Palomo, G. Fernandez-Lorente, J. M. Guisan and R. Fernandez-Lafuente, *Enzyme Microb. Technol.*, 2007, **40**, 1451–1463.
20 B. Krajewska, *Enzyme Microb. Technol.*, 2004, **35**, 126–139.
21 E. Taqieddin and M. Amiji, *Biomaterials*, 2004, **25**, 1937–1945.
22 Z. Ölçer and A. Tanriseven, *Process Biochem.*, 2010, **45**, 1645–1651.
23 M. Matto and Q. Husain, *J. Mol. Catal. B: Enzym.*, 2009, **57**, 164–170.
24 K. F. Fernandes, C. S. Lima, F. M. Lopes and C. H. Collins, *Process Biochem.*, 2004, **39**, 957–962.
25 S. Singh, P. R. Solanki, M. K. Pandey and B. D. Malhotra, *Sens. Actuators, B*, 2006, **115**, 534–541.
26 I. R. W. Z. Oliveira, S. C. Fernandes and I. C. Vieira, *J. Pharm. Biomed. Anal.*, 2006, **41**, 366–372.
27 G. Bayramoglu and M. Y. Arica, *J. Mol. Catal. B: Enzym.*, 2010, **62**, 297–304.
28 D. Brondani, J. Dupont, A. Spinelli and I. C. Vieira, *Sens. Actuators, B*, 2009, **138**, 236–243.
29 S. C. Fernandes, I. R. W. Z. Oliveira and I. C. Vieira, *Enzyme Microb. Technol.*, 2007, **40**, 661–668.
30 K. Kurita, *Prog. Polym. Sci.*, 2001, **26**, 1921–1971.
31 M. Rinaudo, *Prog. Polym. Sci.*, 2006, **31**, 603–632.
32 V. G. Mir, J. Heinämäki, O. Antikainen, O. B. Revoredo, A. I. Colarte, O. M. Nieto and J. Yliruusi, *Eur. J. Pharm. Biopharm.*, 2008, **69**, 964–968.
33 C. K. S. Pillai, W. Paul and C. P. Sharma, *Prog. Polym. Sci.*, 2009, **34**, 641–678.
34 C. Regalado, B. E. García-Almendárez and M. A. Duarte-Vázquez, *Phytochem. Rev.*, 2004, **3**, 243–256.
35 M. Hamid and Khalil-ur-Rehman, *Food Chem.*, 2009, **115**, 1177–1186.
36 G. Battistuzzi, M. Bellei, C. A. Bortolotti and M. Sola, *Arch. Biochem. Biophys.*, 2010, **500**, 21–36.
37 T. L. Poulos, *Arch. Biochem. Biophys.*, 2010, **500**, 3–12.
38 M. Petersen and M. S. J. Simmonds, *Phytochemistry*, 2003, **62**, 121–125.
39 J. Šafra, M. Pospíšilová, J. Honegr and J. Spilková, *J. Chromatogr., A*, 2007, **1171**, 124–132.
40 S. Başkan, N. Öztekin and F. B. Erim, *Food Chem.*, 2007, **101**, 1748–1752.
41 H. Wang, G. J. Provan and K. Helliwell, *Food Chem.*, 2004, **87**, 307–311.
42 M. Öztürk, M. E. Duru, B. Ínce, M. Harmandar and G. Topçu, *Food Chem.*, 2010, **123**, 1352–1356.
43 I. Fecka and S. Turek, *Food Chem.*, 2008, **108**, 1039–1053.
44 Y. Liu, X. Li, Y. Li, L. Wang and M. Xue, *J. Pharm. Biomed. Anal.*, 2010, **53**, 698–704.
45 A. C. Franzoi, J. Dupont, A. Spinelli and I. C. Vieira, *Talanta*, 2009, **77**, 1322–1327.
46 M. Santhiago, R. A. Peralta, A. Neves, G. A. Micke and I. C. Vieira, *Anal. Chim. Acta*, 2008, **613**, 91–97.

47 M. Diaconu, S. C. Litescu and G. L. Radu, *Sens. Actuators, B*, 2010, **145**, 800–806.
48 K. C. Gupta and F. H. Jabrail, *Carbohydr. Res.*, 2006, **341**, 744–756.
49 W. S. W. Ngah, C. S. Endud and R. Mayanar, *React. Funct. Polym.*, 2002, **50**, 181–190.
50 P. Dash and R. W. J. Scott, *Chem. Commun.*, 2009, 812–814.
51 J. R. Carbajal, *Short reference guide of the Program Fullprof: Version 3.5*, Ftp://Charybde.Saclay.Cea.Fr, 2003.
52 D. B. Williams and C. B. Carter, Transmission electron microscopy, in: *A Textbook for Materials Science*, Plenum, N.Y., 1996.
53 L. Zhu, S. Letaief, Y. Liu, F. Gervais and C. Detellier, *Appl. Clay Sci.*, 2009, **43**, 439–446.
54 J. V. B. Kozan, R. P. Silva, S. H. P. Serrano, A. W. O. Lima and L. Angnes, *Anal. Chim. Acta*, 2007, **591**, 200–207.
55 A. Akkaya, C. Altug, N. K. Pazarlioglua and E. Dinckaya, *Electroanalysis*, 2009, **21**, 1805–1810.
56 R. S. Freire, N. Duran and L. T. Kubota, *Anal. Chim. Acta*, 2002, **463**, 229–238.
57 J. Xie, X. Feng, J. Hu, X. Chen and A. Li, *Biosens. Bioelectron.*, 2010, **25**, 1186–1192.
58 S. K. Moccelini, I. C. Vieira, F. Lima, B. G. Lucca, A. M. J. Barbosa and V. S. Ferreira, *Talanta*, 2010, **82**, 164–170.
59 L. Rover Jr., L. T. Kubota and N. F. Höehr, *Clin. Chim. Acta*, 2001, **308**, 55–67.
60 H. B. Yildiz, L. Toppare, Y. H. Gursel and Y. Yagci, *Enzyme Microb. Technol.*, 2006, **39**, 945–948.
61 R. S. Freire, N. Duran and L. T. Kubota, *Talanta*, 2001, **54**, 681–686.
62 R. Yan, F. Zhao, J. Li, F. Xiao, S. Fan and B. Zeng, *Electrochim. Acta*, 2007, **52**, 7425–7431.